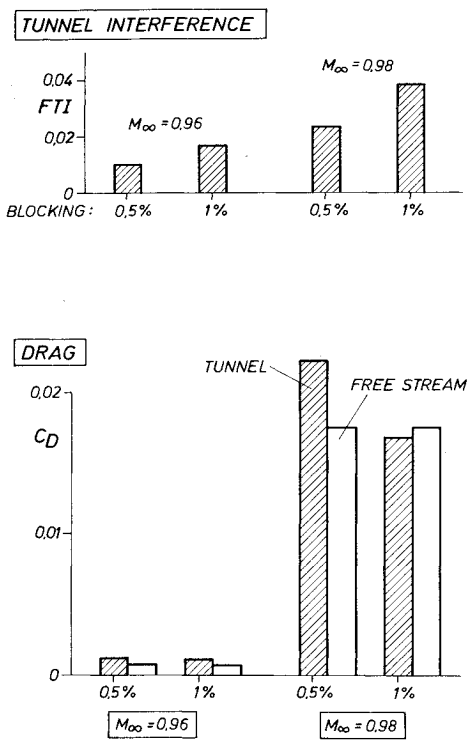

Fig. 3 Typical levels of interference and corresponding pressure drag, realized by searching for "optimal" parameter settings.

ratios (0.5%, 1%). The corresponding inviscid pressure drag of the 0.5% case is shown in the lower part of Fig. 1. It is interesting to note that the drag inflexion points coincide with the minimum FTI. The plenum pressure is zero in Fig. 1, which sets the entrance Mach number to M_∞. The tunnel is fully choked for $M_\infty = 0.98$ while $M_\infty = 0.96$ is at the beginning of the drag-rise phase.

Figure 2 shows what happens to the FTI when the plenum pressure δ and the relative slot depth l/a are varied at $M_\infty = 0.98$ for the 1% area blocking case. The ventilation is the optimal 11% found in Fig. 1. The tunnel interference is considerably reduced by increasing the plenum suction. From Fig. 2 it can be concluded that $\delta = -0.0085$ and 11% ventilation is an "optimal" setting for zero slot depth. This plenum pressure corresponds to an entrance Mach number of 0.99. Figure 3 gives typical examples of the magnitudes to which the tunnel interference can be reduced, when searching for optimal parameter settings for different blocking ratios. It is perhaps paradoxical that the tunnel drag differs more from the reference drag in the 0.5% blocking case than in the 1% case. However, this depends on how the model surface pressures in the two cases are distributed over the body. It should be pointed out that the drag algorithm used in Fig. 3 was improved compared to that applied in Fig. 1. However, the main impression was not altered by this. Work is now ongoing to inversely design slot shapes of varying width that will give almost zero interference on the model. So far, the results are promising and indications are that the tunnel wall boundary layer might play an important role in this.

References

[1] Berndt, S.B., "Inviscid Theory of Wall Interference in Slotted Test Sections," *AIAA Journal*, Vol. 15, Sept. 1977, pp. 1278-1287.

[2] Sedin, Y.C.-J., "Axisymmetric Sonic Flow Computed by a Numerical Method Applied to Slender Bodies," *AIAA Journal*, Vol. 13, April 1975, pp. 504-511.

[3] Karlsson, K.R. and Sedin, Y.C.-J., "The Method of Decomposition Applied in Transonic Flow Calculations," *Lecture Notes in Physics*, Vol. 59, Springer Verlag, New York, 1976, pp. 262-267.

Generalized Velocities in the Outer Region of Hypersonic Turbulent Boundary Layers

Ralph D. Watson*
NASA Langley Research Center, Hampton, Va.

Nomenclature

C = constant in law of the wall, Eq. (2)
k = mixing length slope near wall
R_θ = Reynolds number based on momentum thickness
T = temperature
u = velocity
u^* = generalized velocity [see Eq. (1)], or incompressible velocity
u_τ = shear velocity, $(\tau_w/\rho_w)^{1/2}$
w = wake function, Eq. (4)
y = distance from surface
δ = boundary-layer thickness from pitot survey
η = y/δ_c
ν = kinematic viscosity
Π = velocity defect constant
ρ = density
τ = shear stress

Subscripts

c = edge of wake region
e = edge of boundary layer
w = at wall
t = stagnation value

THE transformation of a compressible turbulent boundary layer to its incompressible counterpart has been studied for many years, primarily to determine the surface shear stress from the velocity profile without resorting to tedious skin friction balance measurements. Boundary-layer transformations are of two types—one in which the y coordinate is modified by Howarth-Dorodnitsyn scaling; the other in which the compressible velocity profile is modified by a density scaling. Many y coordinate transformations are based on Coles' work in Ref. 1, while velocity transformations often stem from Van Driest's mixing length analysis in Ref. 2. A review of both types of transformations, along with extensive references for each, can be found in Ref. 3. The purpose of this Note is to show that the outer portion of the velocity profile of hypersonic turbulent boundary layers can be transformed so that the constants determined by a best fit to the law of the wake[4] are in reasonable agreement with the wake constant for incompressible boundary layers at the same Reynolds number.

Both y transformations and velocity transformations produce velocity profiles which, with the proper choice of τ_w to give u_τ, can be reduced to the incompressible law of the wall. For example, the y transformation of Ref. 5 adequately transformed both adiabatic and cold wall velocity profiles in the wall region for Mach numbers up to about 9. Skin friction coefficients obtained by fitting transformed profiles to the incompressible flow law of the wall were generally in good

Received Aug. 11, 1978; revision received March 5, 1979. This paper is declared a work of the U.S. Government and therefore is in the public domain.

Index category: Boundary Layers and Convective Heat Transfer—Turbulent.

*Aerospace Engineer, Fluid Mechanics Branch, High Speed Aerodynamics Division. Member AIAA.

agreement with measured values, although there appeared to be some disparity between the measured and inferred values at high Mach numbers with wall cooling. In Ref. 6, generalized velocities reduced the wall region of the boundary layer to incompressible form at Mach 11 in helium for T_w/T_t between about 0.3 to 1. Skin friction values inferred from the generalized profiles agreed with direct (skin friction balance) measurements within 6% at near-adiabatic wall conditions and 20% at cold wall conditions. In Ref. 7, hypersonic profiles were reduced using both velocity and y transformations, and it was concluded that the velocity transformation produced a more satisfactory reduction to incompressible form.

Generalized velocities are defined by the following relation:

$$u^* = \int_0^{u'} (\rho/\rho_w)^{1/2}\,du \tag{1}$$

This relation, from the compressible law of the wall, with an assumed Crocco total enthalpy-velocity relation was used in Refs. 7-9 to reduce compressible flow velocity profiles to incompressible profiles. Incompressible velocity profiles in the inner part of a turbulent boundary layer are characterized by the law of the wall, usually written

$$\frac{u^*}{u_\tau} = \frac{1}{k}\ln\left(\frac{yu_\tau}{\nu_w}\right) + C \tag{2}$$

The outer portion of the turbulent boundary layer is characterized by the law of the wake, given by the following equations:

$$\frac{u^* - u_c^*}{u_\tau} = \frac{1}{k}\ln(\eta) + \frac{\Pi}{k}[w(\eta) - 2] \tag{3}$$

where

$$\eta = y/\delta_c, \qquad w(\eta) \simeq 1 - \cos(\pi\eta) \tag{4}$$

For zero pressure gradient turbulent boundary layers at high Reynolds numbers, Π is equal to 0.55 (see Ref. 4). At low Reynolds numbers, Π departs from its equilibrium value, decreasing as the Reynolds number decreases.[1] The thickness δ_c is the value of y at which $\partial(u^*/u_\tau)/\partial(\ln y)$ near the edge of the boundary layer is equal to the slope of the logarithmic profile, k. The value of u^* at δ_c is u_c^*. In Ref. 4, Coles assumed δ_c to be equal to δ and u_c to u_e; however, Bull[10] has emphasized that the distinctions should be preserved.

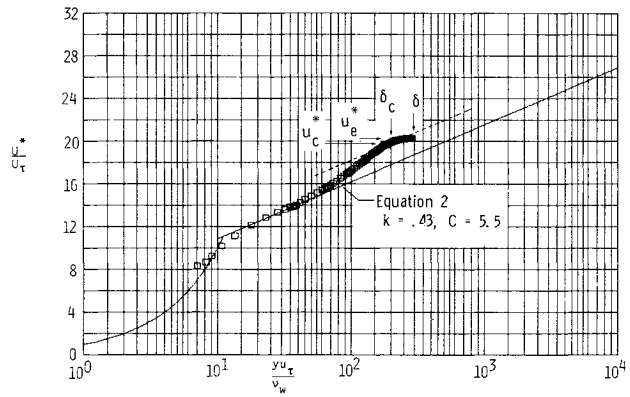

Fig. 1 Generalized velocity profile of Mach 11.4 turbulent boundary layer.

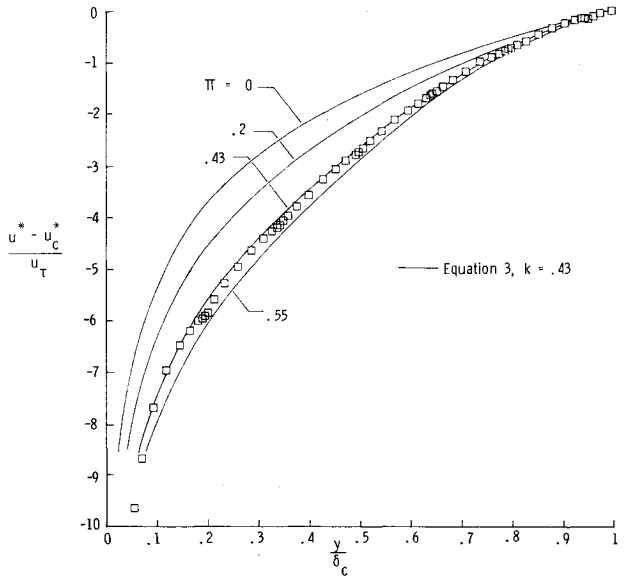

Fig. 2 Generalized velocity defect profile of Mach 11.4 turbulent boundary layer.

Transformations applied to the wake region of turbulent boundary layers do not usually produce the same good agreement with incompressible theory as is found for the wall region.[5,8] One reason, as noted in Ref. 1, is that the outer region is more strongly influenced than the wall region by factors such as external stream turbulence levels and

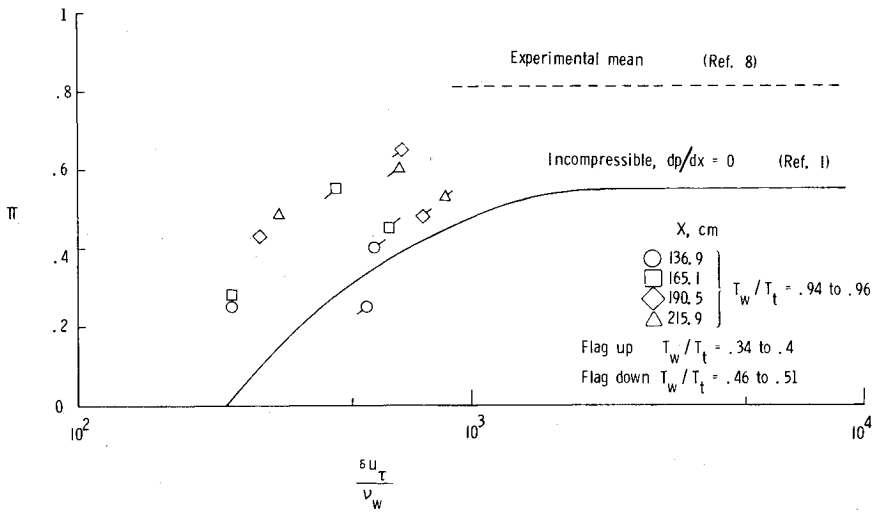

Fig. 3 Variation of Π with $\delta u_\tau/\nu_w$.

departure from two-dimensionality. Another factor which can significantly affect the value of Π that will be obtained from a given profile is the length scale δ_c used to nondimensionalize the y coordinate when plotting the velocity defect profile.

Figure 1 shows a typical generalized velocity distribution in law of the wall coordinates reduced from the tabulated data of Ref. 11. The constants in Eq. (2) ($k=0.43$, $C=5.5$) have been found to be representative of hypersonic turbulent profiles in helium. They are consistent with values to be found in the literature, e.g., $k=0.41$, $C=4.9$ from Ref. 5, and $k=0.43$, $C=6$ from Ref. 8. Noted in the figure are δ, δ_c, u_e^*, and u_c^*. Unlike incompressible and most supersonic turbulent boundary layers, δ/δ_c is 1.5 for the profile shown.

Twelve boundary-layer profiles from Ref. 11 were reduced to generalized velocity defect form using measured skin friction values for calculating u_τ. Values of δ_c for each profile were obtained from plots similar to Fig. 1. The velocity defect region of the boundary layer of Fig. 1 is compared with Eqs. (3) and (4) in Fig. 2 for several values of the wake constant Π. The value of Π for this profile was 0.43, as found by trial-and-error variation of Π until Eq. (3) fits the data. This value is significantly smaller than the high Reynolds number limit of 0.55; however, $\delta u_\tau/\nu_w$ was only 290, indicating the boundary layer to be in the region of low Reynolds number effects. This is evident in Fig. 3 where the variation of Π with $\delta u_\tau/\nu_w$ taken from the tabulation of Ref. 1 for incompressible turbulent boundary layers is shown along with the present Mach 11 data.

Although the present values of Π are greater than Coles' incompressible values, they are lower than the mean value of 0.81 from Ref. 8, and, in addition, exhibit the same trend as incompressible data, a decrease with decreasing $\delta u_\tau/\nu_w$. At $T_w/T_t=0.34$-0.4, Π is closer to the incompressible relation than for the hotter wall data. If inferred instead of measured values of c_f had been used to obtain u_τ, the derived values of Π at cold wall conditions would have been more in agreement with the hot wall data.

All data were originally reduced using δ as the length scale for nondimensionalizing y when plotting the velocity defect. Values of Π obtained by this method were found to be lower than corresponding incompressible values at the same Reynolds number. Since δ_c is the correct length scale to use, only data reduced using δ_c are presented here. The difference in the present data at Mach 11.4 (equivalent to an air boundary layer at Mach 14.7 in terms of density ratio) and the the incompressible is not large when compared with the wide variation in incompressible values of Π found in Ref. 1.

References

[1] Coles, D.C., "The Turbulent Boundary Layer in a Compressible Fluid," R-403-PR, The Rand Corporation, Santa Monica, Calif., 1962.

[2] Van Driest, E.R., "Turbulent Boundary Layer in Compressible Fluids," *Journal of the Aeronautical Sciences*, Vol. 18, 1951, pp. 145-160, p. 216.

[3] Bushnell, D.M., Cary, Jr., A.M., and Harris, J.E., "Calculation Methods for Compressible Turbulent Boundary Layers-1976," NASA SP-422, 1977.

[4] Coles, D.E., "The Law of the Wake in the Turbulent Boundary Layer," *Journal of Fluid Mechanics*, Vol. 1, 1956, pp. 191-226.

[5] Baronti, P.O. and Libby, P.A., "Velocity Profiles in Turbulent Compressible Boundary Layers," *AIAA Journal*, Vol. 4, Feb. 1966, pp. 193-202.

[6] Watson, Ralph D., "Wall Cooling Effects on Hypersonic sitional/Turbulent Boundary Layers at High Reynolds Numbers," *AIAA Journal*, Vol. 15, Oct. 1977, pp. 1455-1461.

[7] Hopkins, E.J., Keener, E.R., Polek, T.E., and Dwyer, H.A., "Hypersonic Turbulent Skin-Friction and Boundary-Layer Profiles on Nonadiabatic Flat Plates," *AIAA Journal*, Vol. 10, Jan. 1972, pp. 40-48.

[8] Danberg, J.E., "A Re-evaluation of Zero Pressure Gradient Compressible Turbulent Boundary Layer Measurements," BRL Rept. No. 1642, U.S. Army Ballistic Research Laboratories, Aberdeen Proving Ground, Md., April 1973, AD-762152.

[9] Maise, G. and McDonald, H., "Mixing Length and Kinematic Eddy Viscosity in a Compressible Boundary Layer," *AIAA Journal*, Vol. 6, Jan. 1968, pp. 73-80.

[10] Bull, M.K., "Velocity Profiles of Turbulent Boundary Layers," *The Aeronautical Journal of the Royal Aeronautical Society*, Vol. 73, Feb. 1969, pp. 143-147.

[11] Watson, R.D., "Characteristics of Mach 10 Transitional and Turbulent Boundary Layers," NASA TP-1243, 1978.

Optimization of Triangular Laced Truss Columns with Tubular Compression Members for Space Application

Chai Hong Yoo*

Marquette University, Milwaukee, Wisc.

Introduction

LARGE space structures built up from a series of long columns to form a stiff skeletal framework are being considered for a number of NASA's future missions[1] such as solar cell platforms or antenna farms. The structural elements of such large space structures are characterized by low loading and minimum gage construction. Euler buckling load is a prominent design consideration. However, minimum gage for production and fabrication frequently is the limiting factor. Due to the obvious reason for minimizing the weight of the structures, optimization is usually considered in terms of minimum weight. As one of the most weight-efficient compression components of large space structures,[2] a tubular laced column is investigated in this study.

The optimization procedures are based on designing for a column with initial imperfections. Initial imperfections associated with columns conceived for space application yield significant implication, since the column behavior is very sensitively affected by these imperfections. These imperfections can result from a number of different causes such as manufacturing in the orbit, thermal gradients, lateral accelerations, and impact during docking. Mikulas[2] made a similar study based on four different column configurations. A comparison of the results of these studies will be shown and the design of diagonals and battens will be discussed.

Truss Geometry

The triangular laced truss column is fabricated with three thin-walled tubular longitudinals placed at each vertex of an isotriangle, which are braced with tubular battens and laced double diagonals in each side of the bay as shown in Fig. 1.

The side length of the isotriangle is readily obtained from the geometry as

$$S=L/N\tan\theta \tag{1}$$

where L is the column length through which the load must be transmitted, N is the number of bays, and θ is the angle between the batten and the diagonal as defined in Fig. 1. The moment of inertia for the truss cross section is:

$$I=A_L S^2/2=A_L L^2/2N^2\tan^2\theta \tag{2}$$

Received Sept. 19, 1978; revision received Feb. 27, 1979.

Index categories: Structural Design; Computational Methods.

*Asst. Professor, Dept. of Civil Engineering.